PHYSICAL REVIEW B VOLUME 25, NUMBER 10 15 MAY 1982

Charge states for H and He moving in an electron gas

F. Guinea and F. Flores
Departamento de Física del Sólido e Instituto de Física del Sólido,
Universidad Autónoma, Madrid-34, Spain

P. M. Echenique
Departamento de Física Fundamental Universidad Central,
Diagonal 541, Barcelona, Spain

(Received 6 October 1981)

A new method for calculating equilibrium charge states for ions moving in a uniform electron gas is proposed. These charge states are obtained in terms of the processes of capture and loss for the level bound to the ion, and these processes are calculated by means of usual many-body techniques. Our method has been applied to H and He, the results showing good agreement with the available experimental evidence.

I. INTRODUCTION

The problem of ions moving in a solid has been the subject of interest since the first years of this century.[1] The energy-loss processes are of great interest from a theoretical and practical point of view.[2] At high velocities ($v >> Z^{2/3}e^2/h$, Z being the atomic number), the ion is stripped of its electronic charge, and its stopping power in its motion across the solid can be obtained from Bethe formula[3] as a function of a few parameters characterizing the ion and the solid.[4] This expression applies for $E \gtrsim 1$ MeV/amu. At low velocities the ion is surrounded by a cloud of electronic charge, and its stopping power can be evaluated by means of a Fermi-Thomas model.[5] This approach, not as accurate as the Bethe method, usually applies for $E \lesssim 10$ keV/amu. At intermediate velocities there is no fundamental theory at all, the problem with this case being that the charge state distribution for the moving ion is not known. Recently, Brandt and co-workers[6,7] have given an effective charge theory to explain stopping powers for those intermediate velocities. This approach is also related to those experiments measuring the charge states of ions emerging from solids.[8,9] Here the number of ions of a given charge leaving the solid are determined as a function of the energy of the ions fired at the target. Although it has not been clearly proven whether those charge states of ions are closely related to their effective charges, it seems to us that a theory determining these charge states would be of great help to the understanding of the stopping powers of ions in solids.

The purpose of this work is to propose a method for calculating equilibrium charges for ions moving in a uniform electron gas within any range of velocities.[10] From the point of view of applied physics, our results are relevant for the intermediate and low velocities of light atoms, a case for which shell corrections can be neglected. In this paper, we only apply our method to protons and He, although an extension to heavier atoms can be easily done.

In our analysis we assume that the ion—H or He—has a bound electron state for the whole range of velocities. Although this assumption will be substantiated by our final results, note that for a proton, Cross[11] has shown that for high velocities an analysis of the charge states of the atom can be done in terms of the processes of capture into, and loss from, the electron level bound to the proton. On the other hand, recent theoretical calculations[12–14] have shown that a proton at rest inside an electron gas can bind two electrons in a stable orbit. As regards He, it is clear that this atom can bind an electron state[15] more easily than H.

In our procedure—extending the Cross approach for high velocities—the charge states of the ion for any range of velocities are determined as a function of the different processes of loss and capture for the electron level bound to the atom. Our method for evaluating these processes is an extension of the many-body techniques[16] to the case of an ion moving inside an electron gas.

In the first step, we determine the wave function and the mean level of the electron bound to the atom by a method which closely follows a recent

©1982 The American Physical Society

work of two of us[15] for impurities in an electron gas. Since a crucial point in this calculation is the screening introduced by the electron gas, we discuss in Sec. II the linear response screening to the nuclear charge. We are interested in analyzing the effect of the screening to the field "felt" by the electron bound to the atom, in order to elucidate how far this field departs from spherical symmetry. For increasing velocities of the ion the results given in Sec. II show that those deviations can be neglected in such a way that the wave function of the electron bound to the atom may be approximated by a wave function with an s symmetry for any velocity.

In Secs. III and IV we discuss our general formalism: First we show how to obtain the wave function of the electron bound to the atom (assuming an s symmetry for the electron state), and then we proceed to determine the charge states for the ion. Our concluding remarks are given in Sec. V.

II. LINEAR RESPONSE THEORY

The linear response theory for a charge moving inside an electron gas has been discussed by many authors in order to analyze plasmon excitations,[17,18] the wake created by a charge along its path,[19,20] and many other effects. It is well established that linear response theory can be applied for the case of charges moving with high velocities in metals; however, for low and intermediate velocities nonlinear effects are important, a charge at rest being a particular case. Although we are more interested in low and intermediate velocities, we discuss the linear theory in this section owing to two main reasons: (1) As stated above we want to find out how far the induced potential around the moving ion departs from the spherical symmetry. For a charge at rest this potential is spherically symmetric, but as its velocity increases the potential loses this symmetry. A strong modification of this type should create an important effect in the electron state bound to the atom. We think that linear theory can give the order of magnitude of these corrections. (ii) On the other hand, linear theory gives the correct limit for charges at high velocities. Having this limit lets us know when nonlinear effects disappear.

It is a well-known result of a linear theory that the screened potential ϕ created by a charge Z moving with velocity $\vec{v}$ is given by:

$$\phi(\vec{k},\omega)=\frac{4\pi Ze^2}{k^2\epsilon(\vec{k},\omega)}\delta(\omega-\vec{k}\cdot\vec{v}) \,, \tag{1}$$

where $\epsilon(\vec{k},\omega)$ is the dielectric function for which a random-phase approximation (RPA) can be used. This result is equivalent to saying that the potential, given in a framework moving with the charge itself, is the following:

$$\phi^V(\vec{k})=\frac{4\pi Ze^2}{k^2\epsilon(\vec{k},\vec{k}\cdot\vec{v})} \,, \tag{2}$$

where instead of the static dielectric function $\epsilon(\vec{k})$, we have now $\epsilon(\vec{k},\vec{k}\cdot\vec{v})$. Then, the potential in real space $\phi^V(\vec{r})$ is given by

$$\phi^V(\vec{r})=\int\frac{d^3k}{(2\pi)^3}\frac{4\pi Ze^2}{k^2\epsilon(\vec{k},\vec{k}\cdot\vec{v})}\exp(i\vec{k}\cdot\vec{r}) \tag{3a}$$

and the induced potential by

$$\phi^{V,I}(\vec{r})=\int\frac{d^3k}{(2\pi)^3}\frac{4\pi Ze^2}{k^2}\left[\frac{1}{\epsilon(\vec{k},\vec{k}\cdot\vec{v})}-1\right]\times\exp(i\vec{k}\cdot\vec{r}) \,. \tag{3b}$$

The use of a RPA for ϵ turns out to be a rather cumbersome calculation that becomes very lengthy and computer time consuming. Accordingly, we have looked for a simple expression for ϵ that could give a reasonable approximation to Eq. (3). To this end we have tried two different approximations to ϵ: (i) First, a plasmon-pole approximation[21]:

$$\epsilon_{\mathrm{pp}}=1-\frac{\omega_p^2}{\omega^2+\omega_p^2-\omega_1^2(k)} \,, \tag{4}$$

where

$$\omega_1^2(k)=\omega_p^2+\frac{k_F^2k^2}{3}+\frac{k^4}{4} \,.$$

(ii) A second approximation is afforded by the dielectric function given in Ref. 22:

$$\epsilon_0=1-\frac{\omega_p^2}{\left[\omega+i\frac{kk_F}{\sqrt{5}}\right]^2-\frac{k^4}{4}} \,. \tag{5}$$

This is similar to the plasmon-pole approximation, but it goes a step further by including some effects associated with the electron-hole pair contribution.[23]

Equations (4) and (5) have been compared with ϵ_{RPA} by calculating $\phi^{V,I}(\vec{r}=0)$ in Eq. (3) with the three dielectric functions. In Fig. 1, $\phi^{V,I}(\vec{r}=0)$ has been plotted for these three cases. From this figure we see that ϵ_0 [Eq. (5)] gives a fair approximation to ϵ_{RPA} in order to obtain $\phi^{V,I}$. On the other

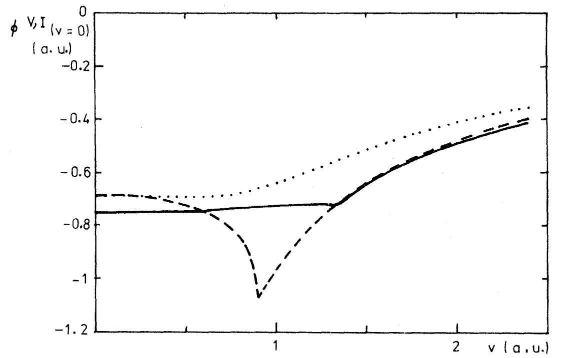

FIG. 1. $\phi^{V,I}(\vec{r}=0)$ (see text), as calculated with three different dielectric functions: full line, ϵ_{RPA}; broken line, ϵ_{pp}; dotted line, ϵ_0 [Eq. (5)].

TABLE I. Induced electron densities upon a moving charge in linear theory. ρ_{RPA} calculated with RPA dielectric function. ρ with the dielectric function described in the text.

v	ρ_{RPA}	ρ
0	1.73×10^{-2}	1.45×10^{-2}
0.25	1.75×10^{-2}	1.47×10^{-2}
0.50	1.73×10^{-2}	1.45×10^{-2}
0.75	1.53×10^{-2}	1.21×10^{-2}
1.00	1.16×10^{-2}	9.9×10^{-3}
1.25	9.3×10^{-3}	8.2×10^{-3}
1.50	7.7×10^{-3}	7.0×10^{-3}
1.75	6.6×10^{-3}	6.1×10^{-3}
2.00	5.8×10^{-3}	5.3×10^{-3}

hand, ϵ_{pp} is not such a good approximation; note, for instance, the minimum given by ϵ_{pp} for $v\simeq1$. Although the curves for $\phi^{V,I}(\vec{r}=0)$ obtained with ϵ_{RPA} and ϵ_{pp} do not differ greatly, the above-mentioned minimum gives some unphysical results when ϵ_{pp} is used to calculate the electronic levels bound by the charge.

Another confirmation of ϵ_0 has been done by obtaining the electron charge density induced on the proton as a function of the velocity of the atom and the electron density. These values have been obtained by using the following equation:

$$\rho^{\mathrm{ind}}(\vec{r})=Ze^2\int\left[\frac{1}{\epsilon(\vec{k},\vec{k}\cdot\vec{v})}-1\right]\times\exp(i\vec{k}\cdot\vec{r})\frac{d^3k}{(2\pi)^3}\,. \quad (6)$$

The results for a RPA calculation are very similar to those obtained by using ϵ_0 [Eq. (5)] in Eq. (6) (see Table I). Owing to this fact and previous results, from now on we shall use ϵ_0 everywhere instead of ϵ_{RPA} for any numerical calculation of an expression having ϵ_{RPA}.

Returning to Eq. (3), one notes that, for $v\neq0$, this equation gives a nonspherical symmetry for the potential $\phi^{V,I}(\vec{r})$. In order to see the importance of the nonspherical components of $\phi^{V,I}(\vec{r})$, we have analyzed the projection of $\phi^{V,I}(\vec{r})$ on the different spherical harmonics. Thus, we can write

$$\phi^{V,I}(\vec{r})=\sum_l\phi_l^{V,I}(r)P_l(\cos\theta')\,, \quad (7)$$

θ' being the angle between $\vec{r}$ and $\vec{v}$, in such a way that $\phi_l^{V,I}(r)$ is given by the following equation:

$$\phi_l^{V,I}(r)=\frac{2Z}{\pi}i^l\int_0^\infty dk\langle\epsilon_0^{-1}(\vec{k},\vec{k}\cdot\vec{v})-1\rangle_l\times j_l(kr)\,, \quad (8)$$

where $\langle\epsilon_0^{-1}(\vec{k},\vec{k}\cdot\vec{v})\rangle_l$ is the projection of the function $\epsilon_0^{-1}(\vec{k},\vec{k}\cdot\vec{v})\equiv\epsilon_0^{-1}(\vec{k},\vec{k}\cdot\vec{v}\cos\theta)$ on the Legendre polynomial $P_l(\cos\theta)$.

In Fig. 2 we have plotted $\phi_s^{V,I}(r)/Z$, $\phi_p^{V,I}(r)/Z$,

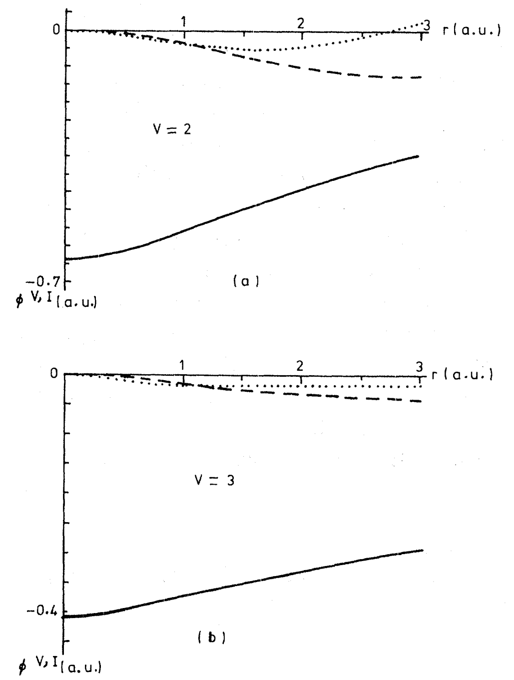

FIG. 2. Different spherical components of the induced potential, $\phi^{V,I}(r)$, for $v=2$ and 3, $r_s=2$. Full line, s component; dotted, p component; broken line; d component.

and $\phi_d^{V,I}(r)/Z$ for different velocities and $r_s=2$. These curves show that $\phi_p^{V,I}(r)$ and $\phi_d^{V,I}(r)$ are much smaller than $\phi_s^{V,I}(r)$ for $r \lesssim 1.5$ in the range of velocities of interest ($v \lesssim 3$). Let us now emphasize that the atomic wave functions bound to the ions (H or He) extend up to distances less than, say, 1.5 a.u. This shows that, as regards the calculation of the bound orbitals, we can neglect any nonsphericity of the potential.

III. GENERAL FORMALISM: WAVE FUNCTION AND MEAN LEVEL

Let us now consider the problem of a light atom moving at low and intermediate velocities inside an electron gas. In this range of velocities the atom is only partially ionized in such a way that any self-consistent treatment of the problem must aim at obtaining the bound states of the atom and its occupation number. In this section we discuss the method we have followed for the determination of wave functions of the electrons bound to the atom as a function of their occupation number. The procedure we have followed for the determination of charge states for the atom will be discussed in Sec. IV.

The method we use in this section closely follows a recent work of two of us for impurities at rest in an electron gas.[15] Some differences, though, must be introduced due to the projectile velocities. First of all, we use a framework moving with the atom (we assume its velocity to be constant, so recoil effects are neglected). From the point of view of this framework the atom is at rest, while the electrons move with an average velocity $(-\vec{v})$; see Fig. 3. In this system of reference, things appear to be stationary; therefore many of the arguments given for an atom at rest can be applied to our present case. Let us briefly discuss the main steps in this procedure and stress the differences introduced by the velocity.

We start with the quasiparticle equation:

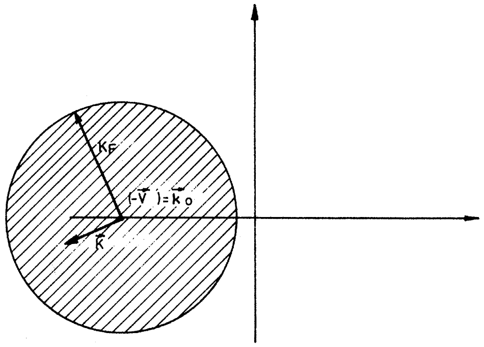

FIG. 3. Shaded region shows the Fermi sphere as seen from a framework moving with the ion.

$$\left[-\tfrac{1}{2}\nabla^2+V_H(\vec{r})+\int d^3r'\Sigma(\vec{r},\vec{r}';E)\right]\psi_i(\vec{r}')=E\psi_i(\vec{r}) \tag{9}$$

where $V_H(\vec{r})$ is the Hartree potential and Σ the self-energy. Assuming Σ is independent of E,[15] we can look for solutions of Eq. (9) in the conduction band in the form

$$\psi_i(\vec{r})=\sum_{\vec{k}} b_{i,\vec{k}}\,|\vec{k}\rangle , \tag{10}$$

where

$$|\vec{k}\rangle=\frac{1}{\sqrt{\mathscr{V}}}\exp(i\vec{k}\cdot\vec{r})-\left\langle s\left|\frac{\exp(i\vec{k}\cdot\vec{r})}{\sqrt{\mathscr{V}}}\right.\right\rangle |s\rangle , \tag{11}$$

where $|\vec{k}\rangle$ is a plane wave orthogonalized to the bound state $|s\rangle$. Moreover, according to the discussion of Sec. II, we take this bound state to be spherically symmetric:

$$|s\rangle=\left[\frac{a^3}{\pi}\right]^{1/2}\exp(-ar) , \tag{12}$$

where a is a variational parameter to be determined by a minimization process. Equation (9) can be written in matrix form by projecting it on the complete basis $\{|s\rangle, |\vec{k}\rangle\}$. It is then an easy matter to obtain the following result:

$$\begin{bmatrix} -E+E_A & 0 \\ 0 & -E+H_M+(E-E_A)S_{MA}S_{AM} \end{bmatrix}\begin{bmatrix} a' \\ b_{\vec{k}} \end{bmatrix}=0 , \tag{13}$$

where

$$E_A=\langle s|\hat{H}|s\rangle ,$$

$$H_M=\left\langle \frac{e^{i\vec{k}'\cdot\vec{r}}}{\mathscr{V}}\left|\hat{H}_M\right|\frac{e^{i\vec{k}\cdot\vec{r}}}{\mathscr{V}}\right\rangle ,$$

and

$$S_{AM}=\left\langle s\left|\frac{e^{i\vec{k}\cdot\vec{r}}}{\mathscr{V}}\right.\right\rangle .$$

This equation allows us to introduce the pseudopotential $(E-H_A)|s\rangle\langle s|$ for the conduction band.

Equation (13) can be used to determine the atomic wave function $|s\rangle$ as well as the perturbation introduced by the atom in the conduction band. However, since the different potentials acting on the free electrons are dependent on the same atomic wave function $|s\rangle$, these equations must be solved self-consistently. This has been achieved in different steps. First, the perturbation introduced by the impurity in the conduction band has been calculated as a function of the parameter a [see Eq. (12)]. Then, the self-energy associated with the atomic wave function has also been obtained as a function of a, and finally this parameter has been calculated self-consistently by minimizing E_A.

This general argument follows closely the case of an impurity at rest.[15] However, some details are different; consider, for example, the calculation of the response function, an essential quantity used for obtaining the perturbation on the conduction-band wave functions due to the entire potential acting on the free electrons. For the perturbed wave functions we can write

$$|\vec{k}\rangle_{\text{pert}}=|\vec{k}\rangle+\sum_{\vec{k}'}\frac{V(\vec{k}-\vec{k}')}{\frac{1}{2}k'^2-\frac{1}{2}k^2}|\vec{k}'\rangle\ , \tag{14}$$

where $V(\vec{k}-\vec{k}')$ is the Fourier transform of the local potential $V(\vec{r})$. Then, the charge induced in the conduction band is given by

$$\delta\rho(\vec{r})=\frac{2}{\mathscr{V}}\sum_{\substack{\kappa<k_F\\ \kappa'>k_F}}\left[\frac{\left[\exp(i\vec{k}\cdot\vec{r})-\dfrac{8a^4\exp(-ar)}{(a^2+k^2)^2}\right]\left[\exp(-i\vec{k}'\cdot\vec{r})-\dfrac{8a^4\exp(-ar)}{(a^2+k'^2)^2}\right]V(\vec{k}-\vec{k}')+\text{c.c.}}{\frac{1}{2}k'^2-\frac{1}{2}k^2}\right]. \tag{15}$$

The main difference with the static case appears in the values taken by $\vec{k}$ and $\vec{k}'$, $\kappa=|\vec{k}-\vec{k}_0|<k_F$ and $\kappa'=|\vec{k}'-\vec{k}_0|>k_F$ (see Fig. 3). Equation (15) can be transformed by means of the change $\vec{\kappa}\rightarrow-\vec{\kappa}$ and $\vec{\kappa}'\rightarrow-\vec{\kappa}'$ (see Fig. 3) applied to the complex conjugate term. In this way, we get the following result:

$$\begin{aligned}
\delta\rho(\vec{q})=\;&\chi_0(\vec{q},-\vec{k}_0\cdot\vec{q})V(\vec{q})\\
&-\frac{1}{\mathscr{V}}\sum_{\substack{\kappa<k_F\\ \kappa'>k_F}}\frac{16\pi a^5}{(a^2+|\vec{\kappa}'+\vec{k}_0^2|^2)^2(a^2+|\vec{\kappa}+\vec{k}_0+\vec{q}|^2)^2}\,\frac{V(\vec{q}')}{\frac{1}{2}\kappa^2-\frac{1}{2}\kappa'^2+\vec{q}'\cdot\vec{k}_0}\\
&-\frac{1}{\mathscr{V}}\sum_{\substack{\kappa<k_F\\ \kappa'>k_F}}\frac{16\pi a^5}{(a^2+|\vec{\kappa}'-\vec{k}_0|^2)^2(a^2+|-\vec{\kappa}+\vec{k}_0+\vec{q}|^2)^2}\,\frac{V(\vec{q}')}{\frac{1}{2}\kappa^2-\frac{1}{2}\kappa'^2-\vec{q}'\cdot\vec{k}_0}\\
&+\frac{1}{\mathscr{V}}\sum_{\substack{\kappa<k_F\\ \kappa'>k_F}}\frac{128\pi a^9}{(a^2+|\vec{\kappa}'+\vec{k}_0|^2)^2(a^2+|\vec{\kappa}+\vec{k}_0|^2)^2}\,\frac{1}{(4a^2+q^2)^2}\,\frac{V(\vec{q}')}{\frac{1}{2}\kappa^2-\frac{1}{2}\kappa'^2+\vec{q}'\cdot\vec{k}_0}\\
&+\frac{1}{\mathscr{V}}\sum_{\substack{\kappa<k_F\\ \kappa'>k_F}}\frac{128\pi a^9}{(a^2+|\vec{\kappa}'-\vec{k}_0|^2)^2(a^2+|\vec{\kappa}-\vec{k}_0|^2)^2}\,\frac{1}{(4a^2+q^2)^2}\,\frac{V(\vec{q}')}{\frac{1}{2}\kappa^2-\frac{1}{2}\kappa'^2-\vec{q}'\cdot\vec{k}_0}\ ,
\end{aligned} \tag{16}$$

where $\vec{q}'=\vec{\kappa}'-\vec{\kappa}$, and $\chi_0(\vec{q},\omega)$ is the RPA polarizability

$$\chi_0(\vec{q},\omega)=\frac{2}{\mathscr{V}}\sum_{\substack{\kappa<k_F\\ \kappa'=|\vec{q}+\vec{\kappa}|>k_F}}\left[\frac{1}{\frac{1}{2}\kappa^2-\frac{1}{2}\kappa'^2-\omega}+\frac{1}{\frac{1}{2}\kappa^2-\frac{1}{2}\kappa'^2+\omega}\right]. \tag{17}$$

Equation (16) can be further simplified by substituting some factors in this equation by an appropiate interpolation between the limits $k_0\rightarrow 0$ and ∞. For example, the factor $1/(a^2+|\vec{\kappa}'+\vec{k}_0|^2)$ has been approximated by $1/(a^2+k_F^2+k_0^2)$, since for $k_0\rightarrow 0$ it can be substituted by $1/(a^2+k_F^2)$ (see Ref. 15), and for $k_0\rightarrow\infty$ it behaves like $1/k_0^2$. It is worth mentioning that the corrections introduced by the orthogonalization hole, collected in the last four terms of Eq. (16), are only important for small v and for a not much larger than k_F. The main virtue of the proposed approximation for the different factors appearing in Eq. (16) is that it gives the right limit for v going to zero,[15] the velocity region for which the orthogonalization hole effects are not negligible.

With this kind of approximation, Eq. (16) yields

$$\begin{aligned}\delta\rho(\vec{q}) &= \chi_0(\vec{q},-\vec{k}_0\cdot\vec{q})V(\vec{q})\\ &\quad+\left[\frac{64\pi a^9}{(a^2+k_F^2+k_0^2)^4(4a^2+q^2)}-\frac{8\pi a^5}{(a^2+k_F^2+k_0^2)^2[(a^2+q^2+k_F^2+k_0^2)^4-4q^2(k_F^2+k_0^2)]}\right]\\ &\quad\times\sum_{q'<2k_F}\chi_0(\vec{q}\,',-\vec{k}_0\cdot\vec{q}\,')V(\vec{q}\,') \,. \end{aligned} \tag{18}$$

Equation (18) and the fundamental equation relating the potential with the charge,

$$V(\vec{q})=V^0(\vec{q})+\frac{4\pi}{q^2}\delta\rho(\vec{q}) \,, \tag{19}$$

allows us to obtain the screened pseudopotential,

$$V(\vec{q})=\frac{V^0(\vec{q})}{\epsilon(\vec{q},-\vec{q}\cdot\vec{k}_0)}+\frac{4\pi}{q^2}\frac{f(q)}{\epsilon(\vec{q},-\vec{q}\cdot\vec{k}_0)}\frac{\displaystyle\sum_{q<2k_F}\left[\frac{1}{\epsilon(\vec{q},-\vec{q}\cdot\vec{k}_0)}-1\right]V^0(q)}{\displaystyle 1+\sum_{q<2k_F}\left[\frac{1}{\epsilon(\vec{q},-\vec{q}\cdot\vec{k}_0)}-1\right]f(q)} \,, \tag{20}$$

where

$$f(q)=\frac{64\pi a^9}{(a^2+k_F^2+k_0^2)^4(4a^2+q^2)}-\frac{8\pi a^5}{(a^2+k_F^2+k_0^2)^2[(a^2+q^2+k_F^2+k_0^2)^2-4q^2(k_F^2+k_0^2)]} \,, \tag{21a}$$

and

$$\epsilon(\vec{q},-\vec{q}\cdot\vec{k}_0)=1-\frac{4\pi}{q^2}\chi_0(\vec{q},-\vec{q}\cdot\vec{k}_0) \,. \tag{21b}$$

Equation (20) defines the screened potential as a function of the projectile velocity measured by $\vec{k}_0$. Having obtained this potential, we can now proceed to discuss how we have defined the energy of the atomic orbital and calculated the parameter a.

As regards the Hartree potential we have included the same interactions discussed in Ref. 15 with the changes introduced by the velocity. For instance, the screened electron-proton interaction must now be obtained by Eq. (20), as well as the electron-electron interaction and the interaction with the orthogonalization hole. In order to obtain the Hartree interaction between the bound orbital and the charge induced by the pseudopotential, $(E-E_A)\,|s\rangle\langle s\,|$, we have approximated this nonlocal potential by the local one:

$$V(\vec{k},\vec{k}')=\begin{cases}(E_F-E_A)\dfrac{64\pi a^5}{(a^2+k_F^2+k_0^2)} & \text{for } |\vec{k}-\vec{k}'|<2k_F\\ 0 \text{ for } |\vec{k}-\vec{k}|>2k_F\end{cases} \tag{22}$$

where again we have used an interpolation between the limits $k_0\to 0$ and ∞. This approximation is similar to that proposed above to simplify Eq. (16), and it has similar advantages since the effects introduced by this pseudopotential on the bound orbital are only important for the limit of low velocities. Moreover, the same type of approximation has been used in other Hartree interactions; they will not be discussed here as the terms involved give minor contributions to this energy.

For the exchange and correlation contributions to E_A, we have followed the simple approximation proposed by Hedin.[24] In this approximation

$$\Sigma(\vec{r},\vec{r}\,';\omega)\simeq -\langle N\,|\,\psi^{\dagger}(\vec{r})\psi(\vec{r}\,')\,|\,N\rangle W(\vec{r},\vec{r}\,';\omega=0)+\tfrac{1}{2}\delta(\vec{r}-\vec{r}\,')W_p(\vec{r},\vec{r}\,';\omega=0)\ . \tag{23}$$

where the first term represents the screened exchange interaction and the second one the Coulomb hole term that can be associated with an adiabatic buildup of the interactions (see Ref. 15). In Eq. (23) W, the screened interaction, is related to W_p, the induced potential, by $W=e^2/|r-r'|+W_p$.

Projecting Eq. (23) on the bound orbital $|s\rangle$, we get the exchange and correlation interaction associated with this state. By using Eq. (20) we can get W and W_p, this equation defining these contributions as a function of the projectile velocity.

Once we have defined the different interactions associated with the bound orbital, we can obtain a and E_A, the atomic wave function [Eq. (12)] and its mean energy, as a function of the projectile velocity and the occupation number N_A for the bound orbital. In Tables II and III, we give a and E_A as a function of v for $N_A=0$, 0.5, and 1 and $r_s=2$ for H and He. For $v=0$ and $N_A=1$ we recover the results given in Ref. 15, although some minor differences appear due to the different dielectric functions used in both cases. On the other hand, as v increases the interaction between the bound orbitals and the electron gas decreases in such a way that a and E_A tend, for $N_A=0$ and 1, to the following values: For H,

$$a=1\text{ a.u.},\quad E_A=-0.5\text{ a.u.},\quad N_A=0$$

$$a=0.6875\text{ a.u.},\quad E_A=-0.021\text{ a.u.},\quad N_A=1\ .$$

For He,

$$a=2\text{ a.u.},\quad E_A=-2\text{ a.u.},\quad N_A=0$$

$$a=1.6875\text{ a.u.},\quad E_A=-0.896\text{ a.u.},\quad N_A=1\ .$$

Note that the differences between these limiting values for a and those given in Tables II and III are a measure of the nonlinear interaction existing between the ion and the electron gas. As was dis-

TABLE II. Values of the exponent a and the energy level E_A relative to the bottom of the band for various occupancies ($r_s=2$). H atom. (Atomic units.)

H	$N_A=0$	$N_A=0.5$	$N_A=1$
$v=0$	$a=0.90$	$a=0.80$	$a=0.76$
	$E_A=-0.106$	$E_A=-0.050$	$E_A=-0.046$
$v=0.2$	$a=0.88$	$a=0.78$	$a=0.72$
	$E_A=-0.096$	$E_A=-0.043$	$E_A=-0.036$
$v=0.4$	$a=0.86$	$a=0.72$	$a=0.76$
	$E_A=-0.075$	$E_A=-0.028$	$E_A=-0.012$
$v=0.6$	$a=0.80$	$a=0.68$	$a=0.54$
	$E_A=-0.048$	$E_A=-0.009$	$E_A=-0.004$
$v=0.8$	$a=0.72$	$a=0.66$	$a=0.52$
	$E_A=-0.027$	$E_A=-0.008$	$E_A=-0.009$
$v=1$	$a=0.74$	$a=0.70$	$a=0.58$
	$E_A=-0.027$	$E_A=-0.008$	$E_A=0.010$
$v=1.2$	$a=0.82$	$a=0.76$	$a=0.70$
	$E_A=-0.041$	$E_A=-0.021$	$E_A=0.011$
$v=1.4$	$a=0.86$	$a=0.80$	$a=0.74$
	$E_A=-0.063$	$E_A=-0.021$	$E_A=0.011$
$v=1.6$	$a=0.90$	$a=0.82$	$a=0.74$
	$E_A=-0.096$	$E_A=-0.034$	$E_A=0.006$
$v=1.8$	$a=0.92$	$a=0.82$	$a=0.72$
	$E_A=-0.125$	$E_A=-0.046$	$E_A=0.005$
$v=2$	$a=0.94$	$a=0.82$	$a=0.72$
	$E_A=-0.184$	$E_A=-0.060$	$E_A=0.001$

TABLE III. Same as Table II, He atom.

He	$N_A=0$	$N_A=0.5$	$N_A=1$
$v=0$	$a=1.88$	$a=1.78$	$a=1.60$
	$E_A=-0.914$	$E_A=-0.748$	$E_A=-0.509$
$v=0.5$	$a=1.88$	$a=1.76$	$a=1.60$
	$E_A=-0.874$	$E_A=-0.615$	$E_A=-0.450$
$v=1$	$a=1.90$	$a=1.74$	$a=1.72$
	$E_A=-0.897$	$E_A=-0.639$	$E_A=-0.439$
$v=1.5$	$a=1.93$	$a=1.80$	$a=1.67$
	$E_A=-1.098$	$E_A=-0.778$	$E_A=-0.540$
$v=2$	$a=1.96$	$a=1.82$	$a=1.7$
	$E_A=-1.252$	$E_A=-0.906$	$E_A=-0.621$
$v=2.5$	$a=1.97$	$a=1.84$	$a=1.7$
	$E_A=-1.327$	$E_A=-0.969$	$E_A=-0.658$
$v=3$	$a=1.98$	$a=1.84$	$a=1.7$
	$E_A=-1.456$	$E_A=-1.090$	$E_A=-0.682$

cussed in Ref. 15, nonlinear effects are included in our calculation through the variational calculation of a; according to Tables II and III these nonlinear effects become small for $v\sim2.5$ a.u. ($r_s=2$). For this velocity we shall see in the next paragraph that N_A is also small, so that with a fair approximation we can say that for greater velocities the interaction between the ion and the electron gas can be obtained by means of a linear response theory.

In addition, it is worth mentioning that the variational parameter a is very slightly dependent on most of the input data discussed above. Note the small changes that Tables II and III show for a. In general, the crucial factor introducing most of the changes in this variational parameter is the orthogonalization hole, and its effect appears mainly through the dielectric function [Eq. (20)] and its Hartree interaction with the bound orbital. As regards E_A, the changes shown in Tables II and III are important due to the contribution coming from the linear screening associated to the interaction between the nucleus and the bound orbital, a contribution giving most of the E_A changes at high velocities. Let us also mention that the major source of error for E_A comes from the approximation given by Eq. (23) for the exchange and correlation interaction and from the variational method itself; from our experience with the static case,[15] we think that this error is around a few tenths of eV's. At this point, it could be of interest to comment that the dielectric function given by Eq. (5) represents a substantial improvement over the plasmon-pole approximation for velocities around $v\simeq1$. Thus, the use of the plasmon-pole approximation could introduce errors as great as 1 eV for E_A.

IV. GENERAL FORMALISM: CHARGE STATES

Once that a and E_A have been determined as a function of N_A, we proceed to calculate the density of states associated to the electron bound to the atom. Our final aim is to determine N_A self-consistently. To this end, we use many-body techniques adapted to our present case. The crucial quantity is the self-energy as given by the RPA approximation[16]

$$\Sigma(\vec{r},\vec{r}\,';\omega)=\frac{i}{2\pi}\int e^{i\eta\omega'}G(\vec{r},\vec{r}\,';\omega+\omega')\times W(\vec{r},\vec{r}\,';\omega)d\omega' , \tag{24}$$

where $G(\vec{r},\vec{r}\,';\omega)$ is the causal Green's function and $W(\vec{r},\vec{r}\,';\omega)$ the causal screened interaction. It is of interest to consider Eq. (24) for a homogeneous electron gas when the framework is moving with a velocity $\vec{v}$. In Appendix A we prove that this self-energy is related to the self-energy for a framework at rest, Σ^0, by means of the following equation:

$$\Sigma(\vec{k},\omega)=\Sigma^0\left[\vec{k}+\vec{v},\omega+\frac{v^2}{2}+\vec{k}\cdot\vec{v}\right] . \tag{25}$$

This is the result we could have expected based on elemental arguments. A particle of momentum $\vec{k}$ and energy ω in the moving framework has the following momentum and energy:

$$\vec{k}'=\vec{k}+\vec{v}\ ,$$

$$\omega'=\omega+\frac{v^2}{2}+\vec{k}\cdot\vec{v}\ ,$$

in the framework at rest.

As in Sec. III, we use Eq. (24) for a framework fixed to the moving atom. Then, the Green's function can be approximated by

$$G(\vec{r},\vec{r}\,';\omega+\omega')=\sum_{\vec{k}}\frac{|\vec{k}',\vec{r}\rangle\langle\vec{k},\vec{r}\,'|}{\omega+\omega'-\frac{1}{2}k^2+i\eta_k}+|s,\vec{r}\rangle\langle s,\vec{r}\,'|\left[\frac{N_A}{\omega+\omega'-E_0-i\eta}+\frac{1-N_A}{\omega+\omega'-E_0+i\eta}\right], \tag{26}$$

where, according to the causal formalism, η_k is a positive infinitesimal for unoccupied states, namely for $|\vec{k}-\vec{k}_0|=\kappa>k_F(\vec{k}_0=-\vec{v})$, while η is a positive infinitesimal also. E_0 is the energy of the bound state as determined from Dyson equation: $\omega=E_M+\Sigma(\omega)$ (see below), an energy which can be different from the mean level E_A as obtained in Sec. III.

On the other hand, the screened interaction $W(\vec{r},\vec{r}\,';\omega)$ can be obtained by using a type of equation analogous to Eq. (20) but generalized to a dynamical case (see Ref. 22). This approximation gives the following equation:

$$W(\vec{q},\omega)=\frac{v_0(\vec{q})}{\epsilon(\vec{q},\omega-\vec{k}_0\cdot\vec{q})}+\frac{4\pi}{q^2}\frac{f(q)}{\epsilon(\vec{q},\omega-\vec{k}_0\cdot\vec{q})}\frac{\displaystyle\sum_{q<2k_F}\left[\frac{1}{\epsilon(\vec{q},\omega-\vec{q}\cdot\vec{k}_0)}-1\right]v_0(q)}{1+\displaystyle\sum_{q<2k_F}\left[\frac{1}{\epsilon(\vec{q},\omega-\vec{q}\cdot\vec{k}_0)}-1\right]f(q)}, \tag{27}$$

where $v_0(q)=4\pi/q^2$ is the bare electron-electron interaction.

Equations (24), (26), and (27) define the whole self-energy; by projecting it on the s level we obtain the following atomic self-energy:

$$\Sigma_A(\omega)=\int d^3r\,d^3r'\langle s,\vec{r}\,|\,\Sigma(\vec{r},\vec{r}\,';\omega)\,|\,s,\vec{r}\,'\rangle\ . \tag{28}$$

In order to analyze the different contributions to Σ_A, we are going to neglect in Eq. (27) the terms associated with the orthogonalization hole, and write

$$W(\vec{q},\omega)\approx\frac{v_0(\vec{q})}{\epsilon(\vec{q},\omega-\vec{k}_0\cdot\vec{q})}\ . \tag{29}$$

In Ref. 22, it was shown that this approximation turns out to be very appropiate in order to calculate the imaginary part of Σ_A. As regards its real part, the effects associated with the orthogonalization hole are important, although its main contribution can be simulated by shifting E_H (the Hartree energy) by a constant; in other words, the dispersive effects introduced by the orthogonalization hole are negligible.

By using Eqs. (29) and (26) we can split the correlation self-energy into four different contributions defined as follows:

$$\Sigma_A^{r,c}(\omega)=\int_0^\infty d\omega''\int_{-\infty}^{\infty}\frac{d^3q}{(2\pi)^3}\sum_{|\vec{k}-\vec{k}_0|<k_F}\frac{4\pi}{q^2}\mathrm{Im}[\epsilon_{\mathrm{RPA}}^{-1}(\vec{q},\omega'')]\frac{\langle s,\vec{r}\,|\,e^{-i\vec{q}\cdot\vec{r}}\,|\,\vec{k},\vec{r}\rangle\langle\vec{k},\vec{r}\,'\,|\,e^{i\vec{q}\cdot\vec{r}\,'}\,|\,s\vec{r}\,'\rangle}{\omega+\omega''-\frac{1}{2}k^2-\vec{q}\cdot\vec{v}-i\eta}\ , \tag{30a}$$

$$\Sigma_A^{r,l}(\omega)=\int_0^\infty d\omega''\int_{-\infty}^{\infty}\frac{d^3q}{(2\pi)^3}\sum_{|\vec{k}-\vec{k}_0|>k_F}\frac{4\pi}{q^2}\mathrm{Im}[\epsilon_{RPA}^{-1}(\vec{q},\omega'')]\frac{\langle s,\vec{r}\,|\,e^{-i\vec{q}\cdot\vec{r}}\,|\,\vec{k},\vec{r}\rangle\langle\vec{k},\vec{r}\,'\,|\,e^{i\vec{q}\cdot\vec{r}\,'}\,|\,s,\vec{r}\,'\rangle}{\omega-\omega''-\frac{1}{2}k^2-\vec{q}\cdot\vec{v}+i\eta}\ , \tag{30b}$$

$$\Sigma_A^{nr,h}(\omega)=\int_0^\infty d\omega''\int_{-\infty}^{\infty}\frac{d^3q}{(2\pi)^3}\frac{4\pi}{q^2}\mathrm{Im}[\epsilon_{\mathrm{RPA}}^{-1}(\vec{q},\omega'')]\frac{\rho_q^2N_A}{\omega+\omega''-\vec{q}\cdot\vec{v}-E_0-i\eta}\ , \tag{30c}$$

$$\Sigma_A^{nr,e}(\omega)=\int_0^\infty d\omega''\int_{-\infty}^{\infty}\frac{d^3q}{(2\pi)^3}\frac{4\pi}{q^3}\mathrm{Im}[\epsilon_{\mathrm{RPA}}^{-1}(\vec{q},\omega'')]\frac{\rho_q^2(1-N_A)}{\omega-\omega''-\vec{q}\cdot\vec{v}-E_0+i\eta}\ , \tag{30d}$$

where $\rho_q=16a^4/[(4a^2+q^2)^2]$ is the Fourier transform of $(a^3/\pi)e^{-2ar}$. Note that Eqs. (30) have been obtained by using the following causal form for $W_p(\vec{r},\vec{r}\,';\omega)$, $W=e^2/|\vec{r}-\vec{r}\,'|+W_p$:

$$W_p(\vec{r},\vec{r}\,';\omega')=\frac{1}{\pi}\int_0^{\infty}d\omega''\int_{-\infty}^{\infty}\frac{d^3q}{(2\pi)^3}\mathrm{Im}[\epsilon_{\mathrm{RPA}}^{-1}(\vec{q},\omega'')]\frac{4\pi}{q^2}\exp[i\vec{q}\cdot(\vec{r}-\vec{r}\,')] \times\left[\frac{1}{\omega'+i\eta+\vec{q}\cdot\vec{v}-\omega''}-\frac{1}{\omega'-i\eta+\vec{q}\cdot\vec{v}+\omega''}\right], \qquad (31)$$

equivalent to Eq. (29).

In Eqs. (30), $\mathrm{Im}\Sigma_A^{r,c}(\omega)$ [or $\mathrm{Im}\Sigma_A^{r,l}(\omega)$] gives the probability by unit time for an electron transition jump from (to) the conduction band to (from) a hole (electron) created in the ion at an ω level; in these processes, an electron-hole pair—or a plasmon—is excited at the same time in the electron gas. On the other hand, $\Sigma_A^{nr,h}(\omega)$ and $\Sigma_A^{nr,e}(\omega)$—the nonrecoil terms—are related to the probability of exciting an electron-hole pair or a plasmon in the electron gas when a hole or an electron are suddenly created in the atom.[22–25]

It is important to note that the imaginary parts of $\Sigma_A^{r,c}(\omega)$ and $\Sigma_A^{nr,h}(\omega)$ are positive, while those of $\Sigma_A^{r,l}(\omega)$ and $\Sigma_A^{nr,e}(\omega)$ are negative; this is a consequence of the fact that $\Sigma_A^{r,c}$ and $\Sigma_A^{nr,h}$ are related to the creation of a hole in the atom. On the other hand, the velocity $\vec{v}$ changes the behavior of these functions dramatically. In particular, for $\vec{v}=0$, $\mathrm{Im}\Sigma_A^{r,c}$ is nonzero only for $\omega<E_F$, while $\mathrm{Im}\Sigma_A^{r,l}$ is nonzero for $\omega>E_F$; for $v\neq0$, these restrictions disappear. In Fig. 4, we show $\mathrm{Im}\Sigma_A^{r,c}(\omega)$ and $\mathrm{Im}\,|\Sigma_A^{r,l}(\omega)|$ for $r_s=2$, and the following velocities: $v=0$, $v=1$ (H) and $v=0$, $v=1.6$ (He) (see Appendix B). From this figure we can see how $\mathrm{Im}\Sigma_A^{r,c}(\omega)$ and $\mathrm{Im}\,|\Sigma_A^{r,l}(\omega)|$ overlap over a region which increases with the velocity. This is one of the main results of our calculation; we will see below how these results are related to the occupation number for the atomic orbital. On the other hand, $\mathrm{Im}\Sigma_A^{nr,h}/N_A$ and $\mathrm{Im}\,|\Sigma_A^{nr,e}|/(1-N_A)$ are symmetric to each other with respect to E_0. In Fig. 5 we show $\mathrm{Im}\Sigma_A^{nr,h}/N_A$ and $\mathrm{Im}\,|\Sigma_A^{nr,e}|/(1-N_A)$ for $r_s=2$ and $v=0,1$ (H), 0,1.5 (He). Note that for $v\neq0$ both quantities also overlap near $\omega=E_0$. It is of interest to note at this point that the results shown in the previous figures (Figs. 4 and 5) have been calculated by using ϵ_0 in Eqs. (30a)–(30d), as given by Eq. (5), instead of ϵ_{RPA}. As was the case earlier in this section we expect this to be a fair approximation to those equations. On the other hand, let us comment on the important role played by the orthogonalized plane waves $|\vec{k},\vec{r}\rangle$ in Eqs. (30). We have checked that it is crucial to include these functions instead of the plane waves, for velocities ranging from 0 to 2

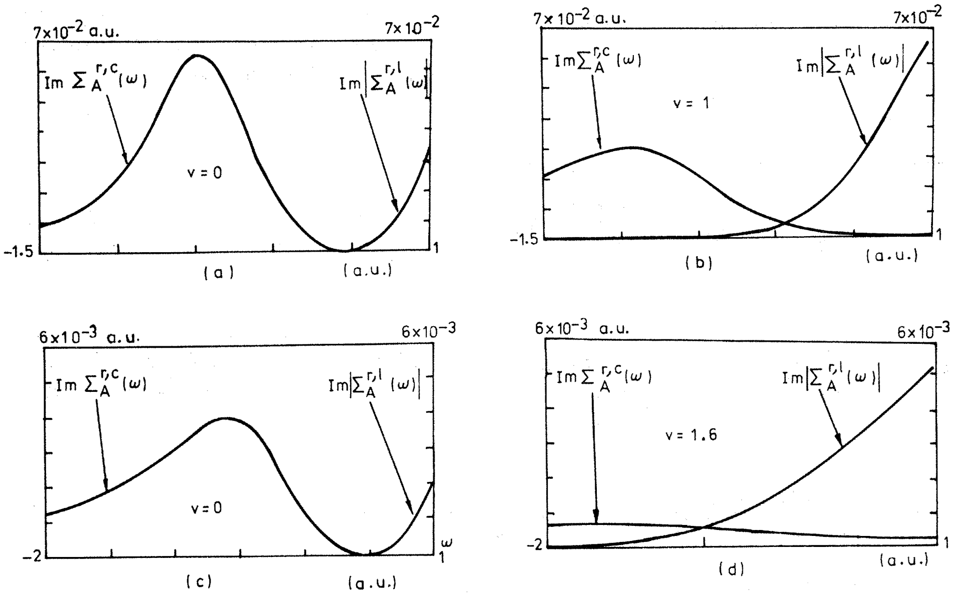

FIG. 4. $\mathrm{Im}\Sigma_A^{r,c}(\omega)$ and $\mathrm{Im}\,|\Sigma_A^{r,l}(\omega)|$ for $r_s=2$, and (a) $v=0$, H; (b) $v=1$, H; (c) $v=0$, He; (d) $v=1.6$, He.

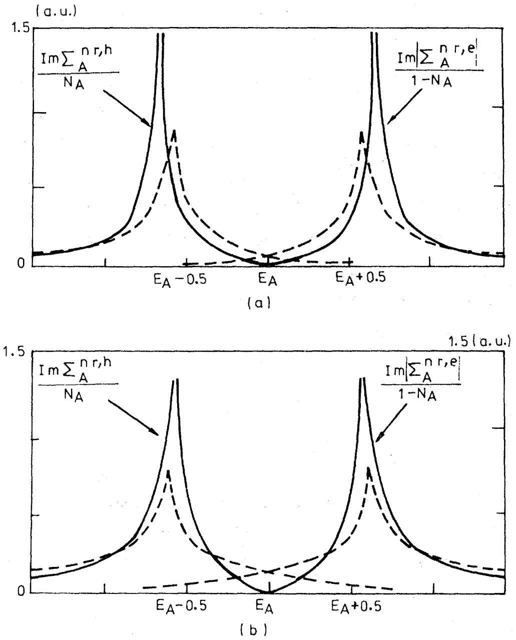

FIG. 5. $\mathrm{Im}\Sigma_A^{nr,h}/N_A$ and $\mathrm{Im}\,|\,\Sigma_A^{nr,e}\,|\,/(1-N_A)$ for $r_s=2$. (a) Full line $v=0$, broken line $v=1$, H. (b) Full line $v=0$, broken line $v=1.6$, He.

a.u. The use of plane waves would introduce very important errors in the different self-energy components, amounting in the most unfavorable cases even to a factor of 10. In other words, the orthogonalization hole introduces substantial modifications in the different probabilities by unit time associated to the transitions between the bound state of the atom and the conduction band.

Now, taking into account the signs associated with the different correlation energies, we can define the density of states associated with the electron bound to the proton as follows:

$$N(\omega)=-\frac{1}{\pi}\mathrm{Im}[\,\omega-E_H-\Sigma_x-\bar{\Sigma}_A^{r,c}(\omega)-\Sigma_A^{r,l}(\omega)-\bar{\Sigma}_A^{nr,h}(\omega)-\Sigma_A^{nr,e}(\omega)]^{-1}\,, \tag{32}$$

where E_H is the Hartree energy associated to the bound electron, Σ_x its exchange energy, and $\bar{\Sigma}$ the complex conjugate of Σ for all the correlation terms.

Equation (32) defines our level, E_0, by means of the following type of Dyson equation:

$$E_0=E_H+\Sigma_x+\mathrm{Re}[\,\bar{\Sigma}_A^{r,c}(E_0)+\Sigma_A^{r,l}(E_0)+\bar{\Sigma}_A^{nr,h}(E_0)+\Sigma_A^{nr,e}(E_0)]\,. \tag{33}$$

Note that Σ is a function of this same level [see Eq. (26) above], which accordingly has to be determined self-consistently. However, in similar problems (Refs. 15 and 22) we have found that E_A, as calculated in Sec. III, is a fair approximation to E_0. Then, according to the discussion given above for the effect of the orthogonalization hole on W [Eqs. (27) and (29)], we have used Eq. (32) with W as given by Eq. (29) and shifted E_H to get $E_0=E_A$ [this is also a fair way of including the orthogonalization hole effects on the density of states given by Eq. (32)].

Having determined the whole density of states and E_0, the problem now is to obtain the occupation number associated to this density. Equation (32) suggests defining the distribution function

$$n(\omega)=\frac{\mathrm{Im}[\bar{\Sigma}_A^{r,c}(\omega)+\bar{\Sigma}_A^{nr,h}(\omega)]}{\mathrm{Im}[\bar{\Sigma}_A^{r,c}(\omega)+\bar{\Sigma}_A^{nr,h}(\omega)+\Sigma_A^{r,l}(\omega)+\Sigma_A^{nr,e}(\omega)]} \tag{34}$$

in such a way that N_A is given by

$$N_A=\int_{-\infty}^{\infty}n(\omega)N(\omega)d\omega\,. \tag{35}$$

Note that $n(\omega)$ is a function of N_A [see Eqs. (30)], and that Eq. (35) must be solved self-consistently for the occupation number, N_A, and the exponent, a, of the orbit bound to the atom.

In general, we have found that Eq. (35) can be approximated by

$$N_A=\frac{\mathrm{Im}[\bar{\Sigma}_A^{r,c}(E_0)]}{\mathrm{Im}[\bar{\Sigma}_A^{r,c}(E_0)+\Sigma_A^{r,l}(E_0)]}\,, \tag{36}$$

this is mainly due to the fact that, as stated above, $\mathrm{Im}\bar{\Sigma}^{nr,h}(\omega)$ and $\mathrm{Im}\Sigma_A^{nr,l}(\omega)$ are symmetric to each other with respect to E_0.

Equation (36) expresses the intuitive result that the occupation number depends on the ratio between the capture and loss cross sections for the atomic level. In Fig. 6 we have drawn for $r_s=2$ and $v=1$ (H), 1.6 (He) the following function:

$$n^r(\omega)=\frac{\mathrm{Im}\bar{\Sigma}_A^{r,c}(\omega)}{\mathrm{Im}[\bar{\Sigma}_A^{r,c}(\omega)+\Sigma_A^{r,l}(\omega)]}\,, \tag{37}$$

which according to Eq. (36) plays the role of a distribution function for the atomic level. It is of interest to note that for $v=0$, $n^r(\omega)$ has a step behavior with a well-defined Fermi level. This is a consequence of the values taken by $\mathrm{Im}\bar{\Sigma}_A^{r,c}(\omega)$ and $\mathrm{Im}\Sigma_A^{r,l}(\omega)$: $\mathrm{Im}\bar{\Sigma}_A^{r,c}(\omega)=0$ for $\omega>E_F$, while $\mathrm{Im}\bar{\Sigma}_A^{r,l}(\omega)=0$ for $\omega<E_F$. However, as v increases, these functions start to overlap (see Fig. 4 above)

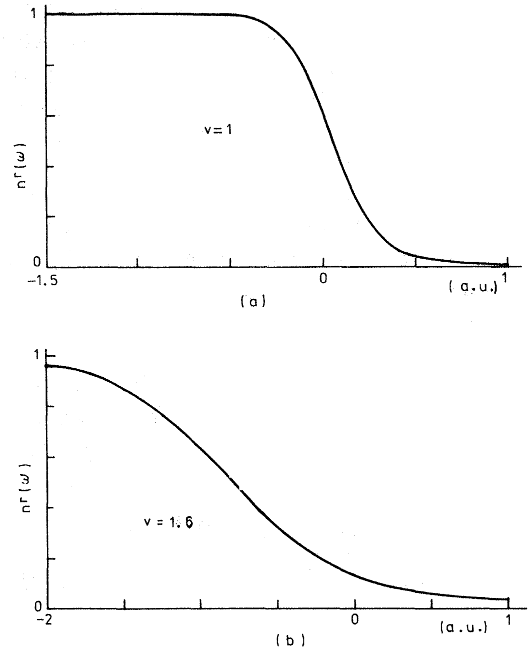

FIG. 6. $n^r(\omega)$ (see text) for $r_s=2$ and (a) $v=1$, H; (b) $v=1.6$, He.

and $n^r(\omega)$ becomes smoother with a general pattern similar to the one given in Fig. 6. Let us now define as the Fermi level E_F for a given velocity v the value of the energy for which $n^r(E_F)=\frac{1}{2}$. Then, the occupation number for the atomic level is determined by the relative position between E_F and E_0. In Fig. 7, E_0 and E_F have been plotted as a function of v for $r_s=2$, H and He; for $v\simeq 1.03$ a.u. and H, $E_0=E_F$, while for $v\simeq 1.63$ a.u. and He, $E_0=E_F$, these being the velocities for which $N_A=\frac{1}{2}$. Note that E_F decreases quickly as a function of v going like $(-v^2/2)$ with respect to the bottom of the band for large values of v; this is a clear consequence of the referential framework which moves with the atom.

We can also define the level broadening by means of the equation

$$\frac{\Gamma}{2}=\mathrm{Im}[\bar{\Sigma}^{r,c}(E_0)+\Sigma^{r,l}(E_0)+\bar{\Sigma}^{nr,h}(E_0)+\Sigma^{nr,e}(E_0)]\ . \qquad (38)$$

The different values of $\Gamma/2$ as a function of v, for $r_s=2$, H and He, have been shown in Fig. 7 by means of the shaded region drawn around the level E_0. It is important to note that, except for a small region near $v_0\simeq 1$ for H, this shaded area does not touch the conduction band; the meaning of this result is that the assumption about the existence of a well-defined atomic level is entirely correct.

It is of interest to make a comment, at this point, about the behavior of $\Gamma/2$ for $v\to 0$. In this limit $\mathrm{Im}\bar{\Sigma}^{nr,h}(E_0)=\mathrm{Im}\Sigma^{nr,e}(E_0)=0$, in such a way that

$$\frac{\Gamma}{2}=\mathrm{Im}[\bar{\Sigma}^{r,c}(E_0)+\Sigma^{r,l}(E_0)]\quad (v=0)\ .$$

This equation defines the Auger line width for the

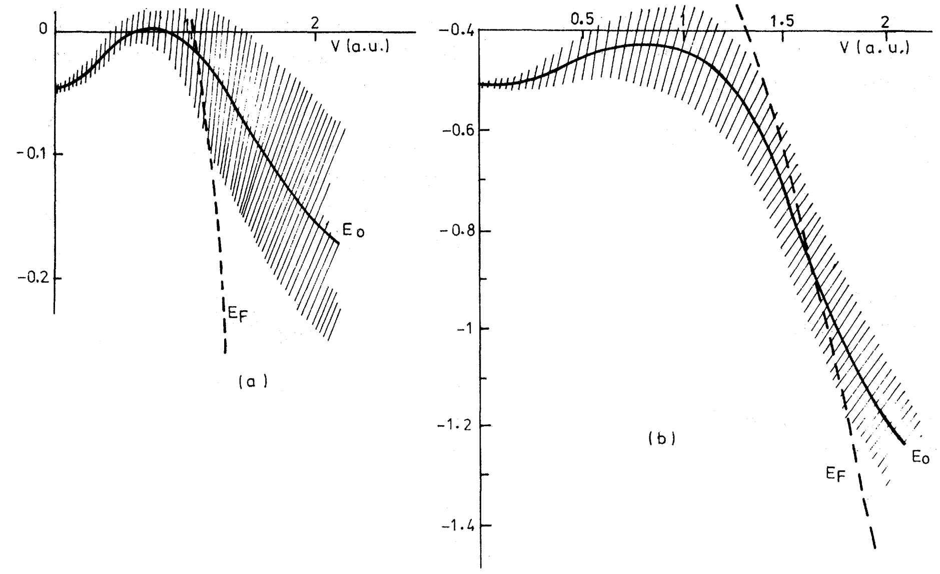

FIG. 7. E_0 and E_F are shown as a function of the velocity of the ion for (a) H and (b) He ($r_s=2$).

core level (see Ref. 22). Now, this line width has a critical dependence on the dielectric function used to calculate Σ. Thus, by using a plasmon-pole approximation $\Gamma/2$ turns out to be zero. However, as discussed in Ref. 22, ϵ_0 [Eq. (5) above] and ϵ_{RPA} give similar line widths for the core level. This is another reason, on top of the discussion given in Sec. II to use Eq. (5) instead of Eq. (4) as a fair approximation to ϵ_{RPA}.

In Fig. 8 we have also shown the atomic density of states (DOS) for $r_s=2$, and $v=1$ (H), 1.6 (He). Note the small structure appearing at $E_0 \pm h\omega_p$. These are the plasmarons[21]; in general, their effects in all the results of this paper are negligible. It is also important to note the broadening associated with the main peak of this atomic DOS; in general, this broadening is small as compared with the width associated with the distribution function $n^r(\omega)$ defined above in Eq. (37) (compare Figs. 6 and 8). Note that this fact reinforces the approximation made in going from Eq. (35) to Eq. (36).

Let us now comment on the degree of accuracy associated with the different approximations made to obtain the results so far given in this paragraph. The main sources of error come from two points: (i) the error in E_0, and (ii) the approximate calculation of the imaginary components of the self-energy as given by Eqs. (30a)–(30d). As regards E_0, from the experience with the static case,[15] we estimate its error to be around ± 0.5 eV, while for the different imaginary components of the self-energy we estimate that they have been calculated with an accuracy better than 70% (see Appendix B). However, the error for the self-energy introduces minor errors in the calculation of $n^r(\omega)$, which accordingly, we think to have obtained with very good accuracy [even a calculation with the values of the self-energy obtained by using plane waves instead of orthogonalized plane wave (OPW) gives a reasonable approximation to $n^r(\omega)$, although each component of Σ itself is then very poorly approximated]. More important is the source of error appearing in the calculation of N_A [Eq. (36)] due to the error in the level, E_0. This can be easily estimated by means of Fig. 6; in this way we obtain that the accuracy of N_A is better than 80%. This shows that $n^r(\omega)$ and N_A have been calculated with a good accuracy, in spite of the lower accuracy appearing in the calculation of E_0 and the components of the self-energy.

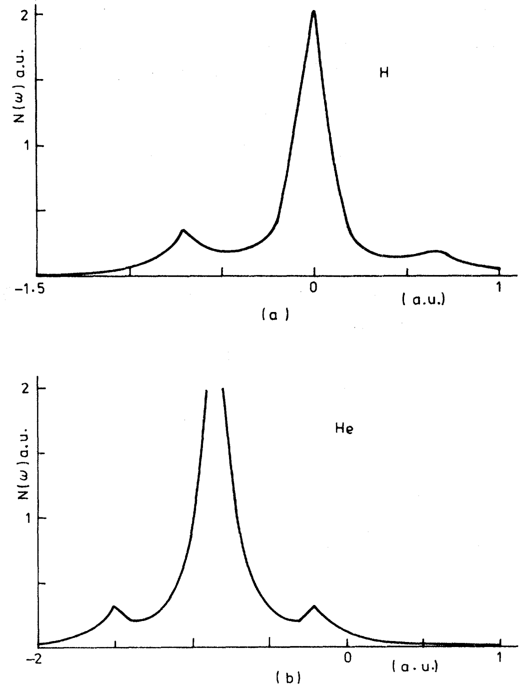

FIG. 8. Atomic density of states, $N(\omega)$, for $r_s=2$ and (a) $v=1$, H; (b) $v=1.6$, He.

Finally, let us obtain the ratio of the fraction of bare atoms to the fraction of atoms with only one electron emerging from the solid. This can be calculated from the occupation number, N_A (shown in Fig. 9 as a function of v), by noting that in our approximation we neglect the intra-atomic electron correlation. Then, $(1-N_A)^2$ gives the fraction of bare atoms, while $2N_A(1-N_A)$ measures the fraction of atoms with only one electron. Note that it would be incorrect to use uncorrelated electrons for the bound orbitals in order to determine the fraction of atoms with two electrons emerging from the solid, since in this case the electron-electron correlation is of primary importance. Moreover, we could expect to have some corrections to the fractions obtained above for bare atoms and atoms with one electron when N_A tends to 1, since in this case the fraction of atoms with two electrons becomes important. Neglecting these corrections, the ratio we are interested in is given by $(1-N_A)/2N_A$. This quantity has been drawn in Fig. 10, for H and He, as a function of v. For H, we show the experimental data given by Phillips[8] for protons emerging from Al. The agreement between our theoretical calculations and these experimental data is rather good, although some discrepancies appear at low velocities. However, note that our calculations give practically a linear relation between $\ln v$ and $\ln(1-N_A)/2N_A$ in agreement with general ar-

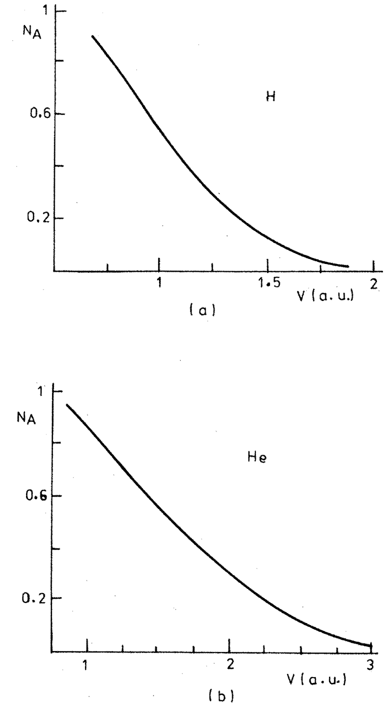

FIG. 9. Shows N_A as a function of v for $r_s = 2$ and (a) H, (b), He.

guments,[26] while Phillips data show a deviation from this linear relation for $v \lesssim 0.8$ a.u. We think that this deviation is partially due to the neglect of intra-atomic correlation quoted above. Surface effects could play a significant role, since for low velocities the atom has enough time to feel the presence of the surface.

V. CONCLUDING REMARKS

We have presented a method to obtain the charge states for ions moving in an electron gas, by means of the techniques commonly used in many-body theory. In our procedure the charge states of the ion are determined as a balance between the processes of loss and capture for the electron state bound to the ion. Our results for protons show a good agreement with the experimental evidence. However, we have remarked that in our approach the intra-atomic electron correlation has been neglected, this being, possibly, the main limitation of the method presented here. For instance, intra-atomic correlation is of primary importance if we are interested in determining the yields associated with the capture of two electrons by a proton, a case that has been overlooked in this paper. Work including the intra-atomic electron correlation in order to obtain the H^- yield is in progress in our laboratory.

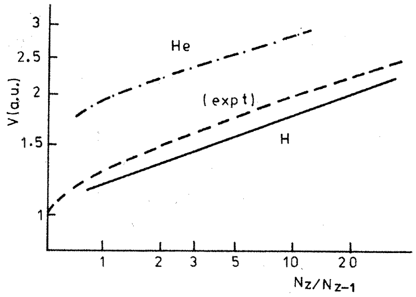

FIG. 10. Ratio between the fraction of bare ions and ions with one electron, N_z/N_{a-1}, as a function of v. Experimental data are for H (broken line.)

APPENDIX A

Here we consider an homogeneous electron gas moving with velocity $(-\vec{v})$. For this case, the Green's-function $G(\vec{r},\vec{r}\,';\omega)$ can be approximated by

$$G(\vec{r},\vec{r}\,';\omega)=\sum_{\kappa}\frac{\exp[i(\vec{\kappa}-\vec{v})\cdot(\vec{r}-\vec{r}\,')]}{\omega-E_{\vec{\kappa}-\vec{v}}+i\eta}\,, \tag{A1}$$

where $\eta = 0^+$ for $\kappa > k_F$ and $\eta = 0^-$ for $\kappa < k_F$. As regards the screened interaction, note that the dielectric function taken from the framework at motion $\epsilon^v(\vec{q},\omega)$ can be related to the usual dielectric function $\epsilon(q,\omega)$ by means of the following equation:

$$\epsilon^v(\vec{q},\omega)=\epsilon(\vec{q},\omega+\vec{q}\cdot\vec{v})\,. \tag{A2}$$

Accordingly we can write

$$\frac{1}{\epsilon^v(\vec{q},\omega)}-1=\frac{1}{\epsilon(\vec{q},\omega+\vec{q}\cdot\vec{v})}-1=\frac{1}{\pi}\int_0^{\infty}d\omega''\,\mathrm{Im}\left[\frac{1}{\epsilon(\vec{q},\omega'')}-1\right]\times\left[\frac{1}{\omega+i\eta+\vec{q}\cdot\vec{v}-\omega''}-\frac{1}{\omega-i\eta+\vec{q}\cdot\vec{v}+\omega''}\right]. \tag{A3}$$

This equation defines the screened interaction $W(\vec{q},\omega)=4\pi/q^2\epsilon^v(\vec{q},\omega)$. Equations (A1) and (A3) yield the following correlation energy:

$$\Sigma_c(\vec{k},\omega)=\int_0^\infty d\omega''\int_{-\infty}^\infty d^3q\frac{4\pi}{q^2}\mathrm{Im}\left[\frac{1}{\epsilon(\vec{q},\omega'')}-1\right] \times\left[\frac{n_{\vec{k}+\vec{v}+\vec{q}}}{\omega+\omega''+i\eta-\vec{q}\cdot\vec{v}-E_{\vec{k}+\vec{q}}}+\frac{1-n_{\vec{k}+\vec{v}+\vec{q}}}{\omega-\omega''+i\eta-\vec{q}\cdot\vec{v}-E_{\vec{k}+\vec{q}}}\right]. \tag{A4}$$

This equation can be transformed into the following result, by means of the equation $E(\vec{k}+\vec{q})=E(\vec{k}+\vec{q}+\vec{v})-\frac{1}{2}v^2-(\vec{k}+\vec{q})\cdot\vec{v}$:

$$\Sigma_c(\vec{k},\omega)=\int_0^\infty d\omega''\int_{-\infty}^\infty d^3q\,\frac{4\pi}{q^2}\mathrm{Im}\left[\frac{1}{\epsilon(\vec{q},\omega'')}-1\right] \times\left[\frac{n_{\vec{k}+\vec{v}+\vec{q}}}{\omega+\omega''+i\eta-E_{\vec{k}+\vec{q}+\vec{v}}+\frac{1}{2}v^2+\vec{k}\cdot\vec{v}} +\frac{1-n_{\vec{k}+\vec{v}+\vec{q}}}{\omega-\omega''-i\eta-E_{\vec{k}+\vec{q}+\vec{v}}+\frac{1}{2}v^2+\vec{k}\cdot\vec{v}}\right]. \tag{A5}$$

This is the correlation energy, $\Sigma_c^0(\vec{k}+\vec{v},\omega+\frac{1}{2}v^2+\vec{k}\cdot\vec{v})$, for an electron of momentum $\vec{k}+\vec{v}$ and energy $\omega+\frac{1}{2}v^2+\vec{k}\cdot\vec{v}$, as given in a framework at rest. A similar argument can be given for the exchange energy, in such a way that, in general,

$$\Sigma(\vec{k},\omega)=\Sigma^0(\vec{k}+\vec{v},\omega+\tfrac{1}{2}v^2+\vec{k}\cdot\vec{v})\ . \tag{A6}$$

APPENDIX B

Details about the method used to calculate $\mathrm{Im}\Sigma_A^{r,c}$ and $\mathrm{Im}\Sigma_A^{r,l}$ are given here. From Eq. (30a) we can write

$$\mathrm{Im}\Sigma_A^{r,c}(\omega)=\pi\int_0^\infty d\omega''\int_{-\infty}^\infty\frac{d^3q}{(2\pi)^3}\sum_k n(\vec{k}-\vec{k}_0)\frac{4\pi}{q^2}\mathrm{Im}[\epsilon_{\mathrm{RPA}}^{-1}(\vec{q},\omega'')]\,|\langle s,\vec{r}\,|e^{-i\vec{q}\cdot\vec{r}}|\,\vec{k},\vec{r}\rangle|^2 \times\delta(\omega+\omega''-\tfrac{1}{2}k^2-\vec{q}\cdot\vec{v})\ , \tag{B1}$$

where

$$n(\vec{k}-\vec{k}_0)=\begin{cases}1 & \text{for}\ |\vec{k}-\vec{k}_0|<k_F\\ 0 & \text{for}\ |\vec{k}-\vec{k}_0|>k_F\ .\end{cases}$$

Let us first assume $|\vec{k},\vec{r}\rangle$ to be a plane-wave function. In this approximation

$$|\langle s,\vec{r}\,|e^{-\vec{q}\cdot\vec{r}}|\,\vec{k},\vec{r}\rangle|^2=\Phi_s^2(\vec{k}-\vec{q})\ , \tag{B2}$$

this equation stressing the dependence of this function on the argument $(\vec{k}-\vec{q})$.

Introducing the new variable, $\vec{q}^*$, defined by

$$\vec{q}^* = \vec{q} + \vec{k}_0 - \vec{k} \,, \tag{B3}$$

Eq. (B1) yields

$$\mathrm{Im}\Sigma_A^{r,c}(\omega) = \pi \int_0^\infty d\omega'' \int_{-\infty}^\infty \frac{d^3q}{(2\pi)^3} \frac{d^3q^*}{(2\pi)^3} \frac{4\pi}{q^2} n(\vec{q}^* - \vec{q}) \mathrm{Im}[\epsilon_{\mathrm{RPA}}^{-1}(\vec{q},\omega'')] \Phi_s^2(\vec{k}_0 - \vec{q}^*) \times \delta(\omega + \omega'' - \tfrac{1}{2}(-\vec{q}^* + \vec{q} + \vec{k}_0)^2 - \vec{q}\cdot\vec{v}) \,. \tag{B4}$$

Now, this equation can be integrated in the angular dependences of $\vec{q}$ and $\vec{q}^*$. Thus

$$\mathrm{Im}\Sigma_A^{r,c}(\omega) = \int_0^\infty d\omega'' \int_0^\infty dq^* \int_0^\infty dq \frac{8a^5 f(q^*,q,\omega'',\omega)}{3\pi^2 qv} \mathrm{Im}[\epsilon_{\mathrm{RPA}}^{-1}(q,\omega'')] \,, \tag{B5}$$

where

$$f(q^*,q,\omega'',\omega) = \begin{cases} 0 & \text{for } S_1 < S_2 \\ \dfrac{1}{(a^2+S_2)^3} - \dfrac{1}{(a^2+S_1)^3} & \text{for } S_2 < S_1 \,, \end{cases}$$

being

$$S_1 = \min|\,|2\omega + 2\omega'' + q^{*2} - (q^* - q)^2|, (q^* + v)^2|$$

$$S_2 = \max|\,|2\omega + 2\omega'' + q^{*2} - (q^* + q)^2|, |2\omega + 2\omega'' + q^{*2} - k_F^2|, (q^* - v)^2| \;.$$

Proceeding in a similar way, we have obtained the following result for $\mathrm{Im}\Sigma_A^{r,l}(\omega)$:

$$\mathrm{Im}\Sigma_A^{r,l}(\omega) = \int_0^\infty d\omega'' \int_0^\infty dq^* \int_0^\infty dq \frac{8a^5 g(q^*,q,\omega'',\omega)}{3\pi^2 qv} \mathrm{Im}[\epsilon_{\mathrm{RPA}}^{-1}(q,\omega'')] \,, \tag{B6}$$

where

$$g(q^*,q,\omega'',\omega) = \begin{cases} 0 & \text{for } t_1 < t_2 \\ \dfrac{1}{(a^2+t_2)^3} - \dfrac{1}{(a^2+t_1)^3} & \text{for } t_2 < t_1 \end{cases}$$

being

$$t_1 = \min|\,|2\omega - 2\omega'' + q^{*2} - (q^* - q)^2|, |2\omega - 2\omega'' + q^{*2} - k_F^2|, (q^* + v)^2| \,,$$

$$t_2 = \max|\,|2\omega - 2\omega'' + q^{*2} - (q^* + q)^2|, (q^* - v)^2| \;.$$

However, Eqs. (B5) and (B6) have been obtained by taking $|\vec{k}\cdot\vec{r}\rangle \sim e^{i\vec{k}\cdot\vec{r}}$. Now, by using an OPW, we must substitute the factor $\langle s,\vec{r}\,|e^{i\vec{q}\cdot\vec{r}}|\,e^{i\vec{k}\cdot\vec{r}}\rangle = \Phi_s(\vec{k}-\vec{q})$ [see Eq. (B2)] by

$$\langle s,\vec{r}\,|e^{i\vec{q}\cdot\vec{r}}|\,\vec{k},\vec{r}\rangle = \Phi_s(\vec{k}-\vec{q}) - \Phi_s(\vec{k})\rho(\vec{q}) \,.$$

In this way, the full expression for $\mathrm{Im}\Sigma_A^{r,c}(\omega)$ is given by

$$\mathrm{Im}\Sigma_A^{r,c}(\omega) = \pi \int_0^\infty d\omega'' \int_{-\infty}^\infty \frac{d^3q^*}{(2\pi)^3} \frac{d^3q}{(2\pi)^3} \frac{4\pi}{q^2} n(\vec{q}^* - \vec{k}_0) \mathrm{Im}[\epsilon_{\mathrm{RPA}}^{-1}(q,\omega'')] \times \Phi_s^2(\vec{q}^* - \vec{q}) \left| 1 - \rho(\vec{q}) \frac{\Phi_s(-\vec{q}^* + \vec{q} + \vec{k}_0)}{\Phi_s(-\vec{q}^* + \vec{k}_0)} \right|^2 \times \delta(\omega + \omega'' - \tfrac{1}{2}(-\vec{q}^* + \vec{q} + \vec{k}_0)^2 - \vec{q}\cdot\vec{v}) \,. \tag{B7}$$

A good approximation to this equation can be obtained by taking

$$\frac{\Phi_s(-\vec{q}^*+\vec{q}+\vec{k}_0)}{\Phi_s(-\vec{q}^*+\vec{k}_0)} \cong 1 \, .$$

We have checked that in the limit $v \to 0$, the most unfavorable case, the accuracy of this approximation for $\text{Im}\Sigma_A^{r,c}$ is better than 70%. Then, the effect of the OPW is embodied in the factor $|1-\rho(\vec{q})|^2$, in such a way that the full expression for $\text{Im}\Sigma_A^{r,c}(\omega)$ [or $\text{Im}\Sigma_A^{r,l}(\omega)$] is given by Eq. (B5) [or (B6)] by including $|1-\rho(q)|^2$ in it. These final expressions, with ϵ_0 substituting to ϵ_{RPA}, have been finally used to compute $\text{Im}\,|\Sigma_A^{r,c}|$ and $\text{Im}\,|\Sigma_A^{r,l}|$.

---

[1] N. Bohr, Philos. Mag. 25, 10 (1903)

[2] *The Stopping and Ranges of Ions in Matter,* edited by J. F. Ziegler (Pergamon, New York, 1977).

[3] H. A. Bethe, Ann. Phys. (Liepzig) 5, 325 (1930).

[4] F. Bloch, Ann. Phys. (Liepzig) 16, 285 (1933)

[5] J. Lindhard, M. Scharff, and H. E. Schiptt, K. Dan. Vidensk. Selsk. Mat. Fys. Medd. 33, No. 14 (1963).

[6] B. S. Yarlagadda, J. E. Robinson, and W. Brandt, Phys. Rev. B 17, 3473 (1978).

[7] S. Kreussler, C. Varelas, and W. Brandt, Phys. Rev. B 23, 82 (1981).

[8] J. A. Phillips, Phys. Rev. 97, 404 (1955).

[9] L. C. Northcliffe, Ann. Rev. Nucl. Sci. 13, 67 (1963).

[10] A preliminary report has been given in Phys. Rev. Lett. 47, 604 (1981).

[11] M. C. Cross, Phys. Rev. B 15, 602 (1977).

[12] C. O. Amblath, V. von Barth, Z. P. Popovic, and M. J. Stott, Phys. Rev. B 14, 2250 (1976).

[13] E. Zaremba, L. M. Sander, H. B. Shore, and J. H. Rose, J. Phys. F 7, 1763 (1977).

[14] J. Arponen and E. Pajanne, J. Phys. C 12, 3013 (1978).

[15] F. Guinea and F. Flores, J. Phys. C 13, 4137 (1980).

[16] L. Hedin and S. Lundquist, in *Solid State Physics,* edited by H. Ehrenreich, R. Seitz, and D. Turnbull (Academic, New York, 1968), Vol. 23, p. 1.

[17] J. Lindhard, K. Dan. Vidensk. Selsk. Mat. Fys. Medd. 28, 8 (1954).

[18] R. H. Ritchie, Phys Rev. 106, 874 (1957).

[19] J. Neufeld and R. H. Ritchie, Phys. Rev. 98, 1632 (1955).

[20] P. M. Echenique, R. H. Ritchie, and W. Brandt, Phys. Rev. B 20, 2567 (1979).

[21] B. Lundquist, Phys. Kondens Mater. 6, 206 (1967).

[22] F. Guinea and F. Flores, J. Phys. C 14, 2965 (1981).

[23] There is a typographical error in the value of ϵ_0 given in Ref. 22; here the square root of 5 has been missed.

[24] L. Hedin, Phys. Rev. A 139, 793 (1965).

[25] P. Nozières and C. T. DeDominics, Phys. Rev. 178, 1097 (1969).

[26] N. Bohr, K. Dan. Vidensk. Selsk. Mat. Fys. Medd. 18, 8 (1948).